

See discussions, stats, and author profiles for this publication at: <https://www.researchgate.net/publication/230677633>

Mechanism for Repair of Thymine Dimers by Photoexcitation of Proximal 8-Oxo-7,8-dihydroguanine

ARTICLE in THE JOURNAL OF PHYSICAL CHEMISTRY A · AUGUST 2012

Impact Factor: 2.69 · DOI: 10.1021/jp305561u · Source: PubMed

CITATIONS

8

READS

14

4 AUTHORS, INCLUDING:



Iwona Wanda Anusiewicz

University of Gdańsk

52 PUBLICATIONS 1,137 CITATIONS

[SEE PROFILE](#)



Piotr Skurski

University of Gdańsk

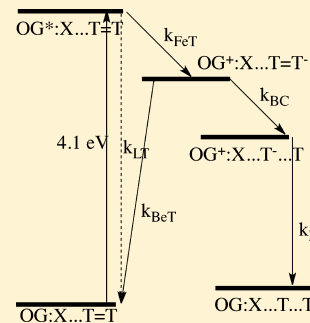
141 PUBLICATIONS 3,383 CITATIONS

[SEE PROFILE](#)

Mechanism for Repair of Thymine Dimers by Photoexcitation of Proximal 8-Oxo-7,8-dihydroguanine

Iwona Anusiewicz,^{†,‡} Iwona Świerszcz,[‡] Piotr Skurski,^{†,‡} and Jack Simons*,[†][†]Department of Chemistry and Henry Eyring Center for Theoretical Chemistry, University of Utah, Salt Lake City, Utah, United States[‡]Department of Chemistry, University of Gdańsk, 80-915 Gdańsk, Poland

ABSTRACT: A wide range of experimental data from earlier studies by other workers are combined with recent data from the Burrows group to interpret that group's thymine dimer ($T=T$) repair rate data for 8-oxo-7,8-dihydroguanine (OG)-containing DNA duplexes. The focus of this effort is to explain (i) how and why the repair rates vary as the sequence location and distance of the OG relative to the $T=T$ is changed and (ii) why the spatial extent over which repair is observed is limited to OG- $T=T$ distances of ~ 6 Å. It is proposed that, if the OG and $T=T$ are within $\sim 5-6$ Å, a Coulomb potential moves the energy of the $OG^+ \cdots T=T^-$ ion-pair state below the photoexcited $OG^* \cdots T=T$ state, even in the absence of full solvent relaxation, thus enhancing forward electron transfer from OG^* to $T=T$ by allowing it to occur as a radiationless internal conversion process rather than by overcoming a solvation-related barrier. The rate of this forward electron transfer is estimated to be $\sim 10\%$ of the decay rate of the photoexcited OG^* . For OG-to- $T=T$ distances beyond $5-6$ Å, electron transfer is still exothermic, but it must occur through solvent reorganization, overcoming an energy barrier, which presumably renders this rate too slow to be detected in the experiments under study here. Once an electron has been injected into the $T=T$, as many other workers have shown, the reaction proceeds through two low-energy barriers first connecting $T=T^-$ to an intermediate in which the $C_5-C_{5'}$ bond of the cyclobutane unit is cleaved, and onward to where the cyclobutane unit is fully broken and two intact thymine sites are established. Our ab initio data show that the energy landscape for these bond cleavages is altered very little by the presence of the proximal OG^+ cation, which therefore allows us to use data from the earlier studies to conclude that it takes ~ 100 ps for complete bond cleavage to occur. The experimentally determined overall $T=T$ repair quantum yield of 1% then allows us to estimate the rate at which an electron is transferred from the $T=T^-$ anion back to the OG^+ cation as 10 times the rate of bond cleavage. The experimental variations in $T=T$ repair rates among several sequences are shown to be reasonably consistent with an exponential OG-to- $T=T$ distance dependence, $e^{-\beta R}$, with a decay parameter of $\beta = 0.6$ Å $^{-1}$. Finally, suggestions are offered for experimental studies that would test the predictions offered here and shed further light on the OG-induced $T=T$ repair mechanism.



I. INTRODUCTION

A. The Experiments We Attempt to Interpret. In a recent experimental study, Nguyen and Burrows¹ studied the repair of thymine dimer (denoted $T=T$) damaged DNA duplexes induced by radiation having energy too low to electronically excite either the $T=T$ site itself or any of the naturally occurring DNA bases but with sufficient energy to excite the 8-oxo-7,8-dihydroguanine (OG) molecule that was placed in various positions relative to the $T=T$ within these duplexes. In Scheme 1, we show at the top the sequence of one such duplex. In the bottom, a schematic representation of the catalytic electron-injection repair mechanism postulated in ref 1 is shown. In ref 2, a similar mechanistic proposal was made in a study of photoactivated repair of $T=T$ dimer damage in DNA with a G-quadruplex being the photoexcited electron donor, again carried out using photons with enough energy to excite the G quadruplex but not the $T=T$ or any of the DNA bases.

In the above sequence and in similar representations throughout this paper, the OG molecule is represented by

the symbol O to avoid confusion with the base guanine G that also occurs in these sequences.

The workers in ref 1 discussed how the widely studied flavoenzyme photolyase acts^{2–5} to repair thymine dimers by absorbing light, undergoing an excitation energy transfer event to form an electronically excited FADH $^-$ anion, and then transferring an electron from the excited FADH $^-$ to the $T=T$ dimer. After this, the two σ bonds in the cyclobutane-like structure of $T=T$ are cleaved, during which process the electron transfers back to the flavin radical.

This kind of mechanism is outlined in Scheme 2 because it can be thought to apply to the case in which OG (actually, in the experiments of ref 1, an OG base paired to A or C, which we denote as OG:X) is excited to a species labeled $OG^*:X$ that has a decay lifetime⁶ having a rate constant k_{LT} and that can

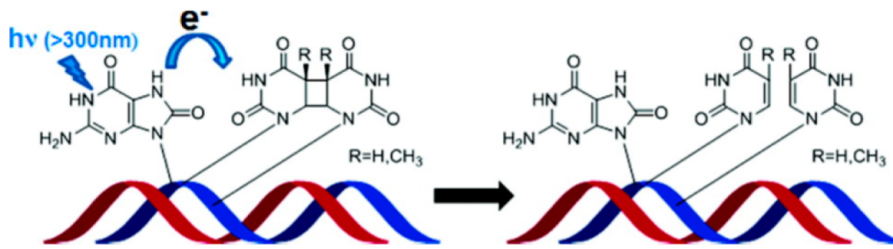
Special Issue: Peter B. Armentrout Festschrift

Received: June 6, 2012

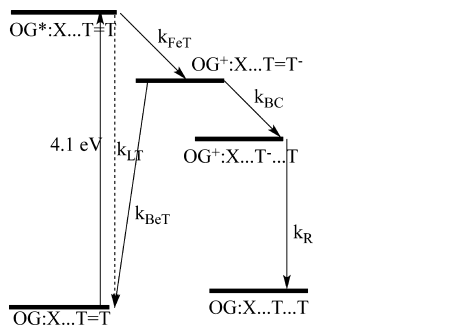
Revised: August 14, 2012

Published: August 15, 2012

Scheme 1. Constructed from Figures 1 and 2 of Ref 1



Scheme 2



forward-transfer an electron to a proximal T=T with a rate characterized by k_{FeT} . The T=T⁻ anion can then undergo C-C bond cleavage⁷ with a rate constant k_{BC} , or it can transfer an electron back to the OG⁺:X cation with a rate characterized by k_{BeT} . Finally, the fraction of molecules that survive both C-C bond cleavages can return an electron to OG⁺:X at a rate characterized by k_R to regenerate the starting material OG:X while leaving the thymine dimer fully repaired.

As we discuss in more detail later, for photolyase,^{8,9} the rate of decay ($k_{LT} \approx 1/1500 \text{ ps}^{-1}$) of the excited FADH⁻ is slower than the rate of forward electron transfer ($k_{FeT} \approx 1/250 \text{ ps}^{-1}$) to T=T, and the rate of back electron transfer ($k_{BeT} \approx 1/1300 \text{ ps}^{-1}$) from T=T⁻ to the FADH radical prior to C-C bond cleavage is slower than the rate ($k_{BC} \approx 1/90 \text{ ps}^{-1}$) of σ-bond cleavage, as a result of which the yield of T=T repair is high and the T=T dimer is largely converted into two intact thymidines. It is the combination of these two rate ratios that makes photolyase such a good T=T repair catalyst.

For OG, it has recently been reported¹⁰ that the quantum yield for T=T cleavage (i.e., the fraction of photons absorbed that result in T=T repair) is ~1%. This would be consistent with either (i) k_{BeT} being ~100 times k_{BC} while k_{FeT} is much larger than k_{LT} , (ii) k_{FeT} being ~1% of k_{LT} while k_{BeT} is considerably smaller than k_{BC} , or (iii) the truth being somewhere between these two limits (e.g., k_{FeT} could be 10% of k_{LT} while k_{BeT} is 10 times k_{BC}). In any event, that fact that the repair quantum yield is much lower than in photolyase means that some of these rate constants must differ substantially between the OG:X and FADH⁻ cases. Later in this paper, we will attempt to demonstrate what the available data and our theoretical studies suggest is most likely the case, but first, it is important to describe in more detail what the experiments of ref 1 showed and how they were performed.

By using a UV light source filtered to exclude photons of wavelength below 300 nm (4.1 eV), the workers of ref 1

excluded any photoexcitation of the T=T moiety or of the A, T, G, or C DNA bases while inducing photoexcitation of the OG. It is important to note that such photons can electronically excite OG (and probably OG:X) but do not have sufficient energy to photoionize isolated OG, whose ionization potential (IP) is in the range of 7.7–8.1 eV,¹¹ or any of DNA's four bases^{11–13} whose IPs are 8.3–9.3 eV. The 4.1 eV photons are also not able to ionize OG:X hydrogen bonded base pairs (where X = C, T, A, or G) which have IPs¹⁴ of 6.8–7.0 eV.

In ref 1, each double-strand sample containing the T=T dimer was subjected to radiation from a 40 W UV lamp, filtered to exclude radiation with energy above 4.1 eV, for a specified time duration, t . The radiated sample was subsequently subjected to HPLC analysis to determine what fraction of the sample remained T=T-damaged and what fraction had been repaired after time t . Analysis of the fraction of repair as a function time displayed first-order kinetics behavior with a rate constant in the range of $1 \times 10^{-2} \text{ min}^{-1}$ at 22 °C.

The rate constant for T=T repair was found to depend upon (i) whether the OG is in the same strand as or in the strand opposite the T=T damage, (ii) whether the OG is to the 3' side of the T=T or toward the 5' side of the T=T, and (iii) how many bases separate the T=T from the OG. We note that Holman et al.¹⁵ also found the T=T repair rate induced by proximal G bases to differ, depending on whether the G was on the 5' (faster) or 3' (slower) side of the T=T.

In Figure 1, we show the rate constants for repair of T=T for various placements of the OG moiety. The sequences used in ref 1 have the OG unit paired with A (where OG is acting as a pyrimidine) or with C (where it is acting as a purine), and, as shown in Figure 1, the repair rate depends on this pairing.

The issues we attempt to address in the present paper include

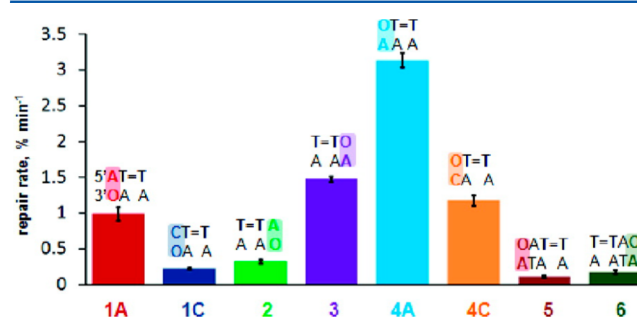


Figure 1. Rates of T=T repair (units of $1 \times 10^{-2} \text{ min}^{-1}$) showing dependence on the location of the OG (labeled O) relative to the T=T (taken from Figure 3 of ref 1).

- (i) On an atomistic level, how does the repair happen; that is, what is the mechanism, and in what ways is it different from how photolyases work? The energy required to remove an electron from OG is much higher than what it takes to remove an electron from FADH^- . Moreover, the $\text{OG}^+:\text{X}\cdots\text{T}=\text{T}^-$ ion pair may be influenced by Coulomb interactions (depending on whether the surrounding medium has time to fully relax and screen this potential) that are not present in the $\text{FADH}\cdots\text{T}=\text{T}^-$ case.
- (ii) Why does the rate depend on the relative positioning of the $\text{T}=\text{T}$ and OG units?
- (iii) Can we estimate the various rates constants in Scheme 2 for the OG case?

It is important to make it clear that our approach is not to carry out full dynamical simulations of the photoexcitation, electron injection, $\text{T}=\text{T}^-$ ring-opening, and back electron transfer processes. To do so is beyond our present computational limits. Moreover, as we attempt to show later, considerations of molecular geometry and electrostatics, combined with the data trends observed in ref 1 and in experiments from other groups, provide sufficient information for us to put forth a reasonable and experimentally testable postulate for how and at what rates OG-induced $\text{T}=\text{T}$ repair takes place.

Having specified what our goals are and are not, it is appropriate to briefly review recent theoretical and experimental findings on thymine dimer anion repair mechanisms and rates when photolyase serves to effect the $\text{T}=\text{T}$ repair. As we discuss later, we believe there are substantial differences between the rates of the various mechanistic steps operative in the photolyase and OG cases, so the following brief review is provided as a foundation for specifying these differences.

B. Review of Selected Recent Experimental and Theoretical Studies on Similar Systems. There have been several cutting-edge theoretical simulations of how the anionic $\text{T}=\text{T}^-$ unit undergoes bond cleavage to form T and T^- . Hassanali et al.^{16,17} carried out ab initio molecular dynamics (AIMD) studies (at the density functional level using plane-wave basis sets) on the anion of a thymine cyclobutane dimer model compound surrounded by explicit water molecules. A statistically significant sample of initial conditions was employed for the trajectories propagated. They found the $\text{C}_5-\text{C}_{5'}$ bond to cleave before the $\text{C}_6-\text{C}_{6'}$ bond, with full cleavage of the cyclobutane unit occurring within several picoseconds. Their free energy surface showed a barrier of ~ 1.5 kcal mol⁻¹ for the transition state leading to cleavage of the $\text{C}_6-\text{C}_{6'}$ bond and a smaller barrier for cleaving the $\text{C}_5-\text{C}_{5'}$ bond. They also observed significant delocalization of the anion's excess electron onto the surrounding water molecules. Earlier, Masson et al.¹⁸ carried out molecular dynamics simulations using a combined quantum/classical (QM/MM) force field (with the QM performed at the density functional level) on a DNA double strand decamer containing the $\text{T}=\text{T}$ damage. They selected seven initial conditions (chosen from a purely classical NPT simulation) to follow the time evolution at the QM/MM level with an electron added to the $\text{T}=\text{T}$ site. These workers also observed full cleavage of the cyclobutane unit in $\text{T}=\text{T}^-$ within a few picoseconds; they estimated the free energy barrier to cleaving the $\text{C}_6-\text{C}_{6'}$ bond to be 2.5 kcal mol⁻¹ or less; and they explained,¹⁹ on the basis of the charge density of the $\text{T}=\text{T}^-$ π^* orbital holding the excess electron, why the $\text{C}_5-\text{C}_{5'}$ bond cleaves before the $\text{C}_6-\text{C}_{6'}$ bond.

On the experimental front and even earlier, Chatgilialoglu et al.²⁰ observed in pulse radiolysis experiments on the thymine dimer anion in water evidence suggesting that both C–C bonds are cleaved within a few picoseconds. These same workers performed density functional calculations on the thymine dimer anion, from which barriers of 1.8 kcal mol⁻¹ and 3.2 kcal mol⁻¹ for cleaving the $\text{C}_5-\text{C}_{5'}$ and $\text{C}_6-\text{C}_{6'}$ bonds, respectively, were obtained. On the basis of these calculations, and using a pre-exponential rate factor of 10^{13} s⁻¹, they estimated the time for cleaving both C–C bonds to be 15–16 ps.

Recently, Liu et al.⁸ used femtosecond-resolved spectroscopic tools to probe (i) the excitation energy transfer to the FADH^- unit, (ii) the electron transfer from FADH^- to the thymine dimer, (iii) the splitting of the cyclobutane unit in the thymine dimer, and (iv) the back electron transfer to the FADH radical. In discussing how the electron moves from the FADH^- to the $\text{T}=\text{T}$, these workers mention the earlier suggestion by Anthony et al.²¹ that an intervening adenine serves to mediate the process. Of most importance to the present study are their findings that (i) cleavage of the two C–C bonds in the thymine dimer anion requires ~ 90 ps, (ii) back electron transfer *prior* to cleaving these two bonds occurs on a slow time scale of 2.4 ns, (iii) return electron transfer after the two C–C bonds are cleaved takes 700 ps, and (iv) the forward electron transfer from FADH^- to $\text{T}=\text{T}$ takes place on a time scale of 250 ps.

More recently, Kao et al.⁹ covalently linked reduced lumiflavin (LFH^-) to a thymine dimer and studied the same kinds of rates as this same group considered in ref 8. For the LFH^- case, they found (i) the cleavage of both C–C bonds to require ~ 435 ps, (ii) back electron transfer *prior* to cleaving both bonds on a time scale of 95 ps, (iii) return electron transfer after the two C–C bonds cleave to require 23 ps, and (iv) the initial electron transfer from LFH^- to $\text{T}=\text{T}$ takes place on a time scale of 79 ps. In ref 9, it is reported that the lifetime of the photoexcited LFH^- is 5.8 ps, whereas that of photoexcited FADH^- is 1500 ps. The most important differences between the findings of ref 9 for LFH^- and those reported in ref 8 for FADH^- appear in the rates of back electron transfer from the $\text{T}=\text{T}^-$ anion to the original source of the excess electron and in the lifetime of the photoexcited species. In FADH^- , the back-transfer rate is ~ 30 times slower than in LFH^- , even though the distances between the electron donor and the $\text{T}=\text{T}$ do not differ considerably. Moreover, the lifetime of the excited FADH^- is much longer than that of LFH^- . In ref 8, a good explanation for these differences is offered on the basis of the structural rigidity of FADH^- within photolyase.

To summarize, it appears that a substantial body of experimental and theoretical work supports a picture when photolyase is operative in which the electron is transferred from FADH^- to $\text{T}=\text{T}$ much faster than the photoexcited FADH^- can decay, after which both C–C bonds break within 90 ps and back electron transfer to the neutral FADH radical is slow enough (both early and late in the $\text{T}=\text{T}^-$ to $\text{T} + \text{T}^-$ rearrangement path) to make the yield of $\text{T}=\text{T}$ repair near unity per electron reaching the $\text{T}=\text{T}$ site. The slow rate of back electron transfer in the FADH ($1/1300$ ps⁻¹) is, as noted above, in contrast with what happens when tethered LFH^- is the electron donor ($1/5.8$ ps⁻¹) and, as will be demonstrated later, also in contrast with the present case when OG is the donor. These differences are important because slow back electron transfer and a long excited state lifetime are important

to achieving high overall efficiency in repairing the T=T damage site.

It should also be mentioned that other recent experimental work²² has shown that T=T repair induced by photoinitiated electron transfer from a nearby G or A base to the T=T site is negligible in comparison with the T=T repair caused by direct photoexcitation of the T=T unit. Photons having energy high enough to excite the T=T produced significantly higher repair than when photons below the T=T excitation threshold were used. This observation would seem to call into question the proposition that photoexcitation of a neutral base (or of OG) followed by electron transfer to T=T can generate appreciable T=T repair. However, in the study of ref 1, photoexcitation of T=T was presumably excluded by filtering out light with energy above 4.1 eV, while T=T repair was still observed (as it was when photoexcitation of a G quadruplex was used² as the putative electron source). The combination of these data suggests that higher-energy photons can directly excite T=T and induce (perhaps more rapid) repair, whereas lower-energy photons can excite other nearby chromophores (e.g., A, G, or OG), which might then transfer an electron to T=T to initiate (perhaps slower) repair.

We have every reason to believe that the results of these modern cutting-edge studies are correct as they relate to T=T repair by photolyase or by tethered LFH⁻. However, in the systems studied in ref 1 that we focus on here, there is at least one difference that we believe merits the extra attention we give it in Section III.

Unlike the photolyase or LFH⁻ cases, in which the electron comes from the negatively charged FADH⁻ or LFH⁻, in the species treated here, the electron comes from the neutral OG^{*}:X. As a result, immediately after injection of an electron from OG^{*}:X to T=T, the T=T⁻ anion experiences a Coulombic interaction with the OG⁺:X cation. In fact, as we show in Section III, this Coulomb potential lowers the energy of the OG⁺:X···T=T⁻ ion pair state relative to the OG^{*}:X···T=T state, which may affect the rate of forward electron transfer. Moreover, depending on how long the T=T⁻ anion exists before undergoing either C-C bond cleavage or back electron transfer to the OG⁺:X cation, this same Coulomb potential may affect these rates. If the time it takes for C-C bond rupture or for the electron to move from T=T⁻ to OG⁺:X is much longer than the ~10 ps it takes the solvent water molecules to reorient, the Coulomb interaction will be highly screened and, thus, should have minimal effect. On the other hand, if the bond rupture or back electron transfer takes on the order of 10 ps or less, the Coulomb interaction will be far less screened and can have an influence. This is why we need to examine the extent to which a Coulomb potential may alter the energy landscape for cleaving the C₅-C_{5'} and/or C₆-C_{6'} using the techniques that we now describe.

II. METHODS

A. The Calculations Performed for the Neutral and Anionic Thymine Dimer. The equilibrium structures of the neutral and anionic thymine dimer were first determined at the Hartree-Fock level (HF) with a 6-31+G(d)^{23,24} basis set that was modified in the following manner to make sure that a proper description of the T=T⁻ anion's singly occupied orbital is achieved. To describe attaching an excess electron to the π* orbital of thymine, we needed to make sure that our atomic orbital basis set produced a π* orbital having a positive energy of 0.25 eV, which is the neutral-anion energy gap that is

experimentally observed. We did so by scaling the exponents of the most diffuse s- and p-type basis functions on the atoms within the thymine ring to produce the lowest π* orbital on thymine with this energy. The stationary-point structures (i.e., transition states, intermediate product with one C-C bond broken, and the final product structure with the two thymine rings reconstituted) were also located using this modified 6-31+G(d) basis set and the HF method. The intrinsic reaction coordinate intrinsic reaction coordinate (IRC) technique^{25,26} was employed to characterize the reaction paths connecting these stationary points.

Having the Hartree-Fock energy profiles (including the stationary points) calculated, we then employed the second-order Møller-Plesset (MP2) perturbation method with a similarly modified 6-31+G(d) basis set to obtain the relevant MP2 energies for all stationary points. Of course, we had to perform an independent orbital exponent scaling of the most diffuse s- and p-type basis functions to achieve an energy of 0.25 eV for the neutral-anion energy gap of the thymine π*-attached state at the MP2 level of theory. To approximate the effect of surrounding solvent molecules and of the remainder of the duplex structure on the electronic energy of the neutral and anionic thymine dimer, we employed the polarized continuum (PCM) solvation model²⁷⁻²⁹ within a self-consistent reaction field treatment, as implemented in the Gaussian09 program.³⁴ Studies of the energy profiles with dielectric constants of 1.0 (gas phase), 2.02 (cyclohexane), 36.64 (acetonitrile), and 78.39 (water) were included to gain appreciation for how strongly the most important aspects of the resulting data (e.g., barrier heights and overall thermochemistry) depend on the solvation strength.

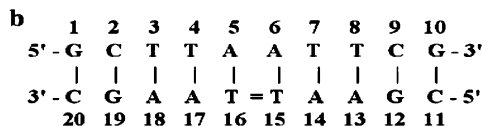
B. Calculations Performed for the DNA Fragment Containing the T=T and OG Moieties. As will be made clear in Section III, we needed to determine that the ion-pair state in which an electron is removed from the OG and transferred to the T=T is lower in energy than the state in which only the OG unit is electronically excited. In particular, we needed to determine this for those sequences that were found to undergo T=T repair. So we carried out ab initio variational (to locate the lowest state of the chosen symmetry) calculations on two model systems designed to simulate the sequences labeled 4A and 3 in Figure 1. We formed these fragment models (each containing six total bases) by using a structure found in the protein database³⁰ crystal structure (1N4E) that contained the T=T unit. Since the structure obtained from the protein database crystal structure did not contain the OG base, we replaced one of 1N4E's adenines proximal to the T=T unit with OG, doing so in either the 3' or 5' direction to generate the two model systems.

For calculating the energies and singly occupied orbitals at the stationary points along the reaction paths, the structure of the T=T unit in the DNA fragment was modified to be as close as possible to that in each stationary point (e.g., starting T=T, transition state, intermediate, and product) determined as described in Section IIA for the isolated thymine dimer anion. Calculations (at both HF and MP2 levels) were carried out using the two-layer ONIOM approach³¹⁻³³ in which the system was divided into two layers treated with different model chemistries. The high layer containing the thymine dimer (T=T) and the OG was treated with the MP2 method using the 6-31+G(d) basis set,^{23,24} whereas the low layer (containing the remaining atoms) was described with the Hartree-Fock method using the 6-31G basis set. To focus on the

$\text{OG}^+ \cdots \text{T}=\text{T}^-$ ion pair state in comparison with the state in which only the OG unit is excited, we performed calculations on the lowest-energy triplet state rather than the singlet state. This strategy allowed us to avoid having the variational calculation collapse and yield the wave function for the ground singlet state in which neither OG nor $\text{T}=\text{T}$ is excited. Because the singly occupied molecular orbitals (SOMOs) of OG^+ and $\text{T}=\text{T}^-$ are weakly coupled (because they are localized on spatially separated fragments), the energy and orbitals we obtained in these triplet-state calculations are expected to be very similar to their singlet-state counterparts. As we show in Section IIIE, for the model systems in which the OG is proximal to the $\text{T}=\text{T}$ site, the lowest-energy triplet states indeed correspond to the $\text{OG}^+ \cdots \text{T}=\text{T}^-$ ion-pair state rather than the state in which only the OG is excited. Moreover, the SOMOs of this state describe (i) an electron in a π orbital on the OG and (ii) an electron in a π orbital of the $\text{T}=\text{T}$. Finally, the PCM solvation model (for the dielectric constant of 2) was used to verify the influence of the solvation strength on the barrier heights, and all of the calculations were performed with the Gaussian09 program.³⁴

III. RESULTS

A. Structural Considerations. Because we do not know the precise internal geometries of the duplex species used in ref 1 and because we think the distances between and the relative orientations of the $\text{T}=\text{T}$ and OG units are important variables if electron ejection from $\text{OG}^*:X$ to $\text{T}=\text{T}$ is operative, we decided to first examine the interbase distances found in a protein database³⁵ crystal structure (1N4E) that contains a $\text{T}=\text{T}$ unit and that has the following sequence:



Two views of this duplex's molecular structure as extracted from the crystal structure data are shown in Figure 2.

Although there clearly are substantial differences between the 1N4E sequence and the sequences employed in ref 1, we think the availability of accurate structural information on the former allows us to make interbase distance and orientation estimates that can guide our studies of the events observed in ref 1.

In Table 1, we show various distances between the $\text{T}=\text{T}$ unit and the nearby bases in the 1N4E crystal structure that we

Table 1. Distances (\AA) from $\text{T}=\text{T}$ to the OG Unit Replacing Various Bases for the Sequence Shown below within 1N4E^a

base replaced by OG	$\text{C}_2\text{T}_3\text{T}_4\text{A}_5\text{A}_6\text{T}_7\text{T}_8\text{C}_9$			$3e^{-\beta(R_{\text{middle}} - 5.4\text{\AA})}$		
	middle distance, \AA	minimum distance, \AA	with $\beta = 0.6 \text{\AA}^{-1}$	repair rates 10^{-2} min^{-1}	quantum yield (%)	
A_{17}	6.6	3.2	1.5	1.5	0.47	
A_{14}	5.4	3.0	3	>3	1.0	
A_{18}	11.2	7.0	0.1	0.2	0.06	
A_{13}	8.6	6.0	0.4	<0.2	0.04	
G_{19}	13.5	9.8	0.02			
G_{12}	12.6	9.0	0.04			
T_4	9.3	4.2	0.3	0.3		
T_7	7.9	3.1	0.7	1		
T_3	11.0	6.8	0.1			
T_8	10.0	6.0	0.2			
C_2	12.2	9.0	0.05			
C_9	12.7	8.8	0.04			
A_5	7.2	2.4	1.0	2		
A_6	7.1	2.5	1.1	0.3		

^aSee text for details. The repair rates come from Figure 3 of ref 1, and the quantum yields for $\text{T}=\text{T}$ repair come from ref 10.

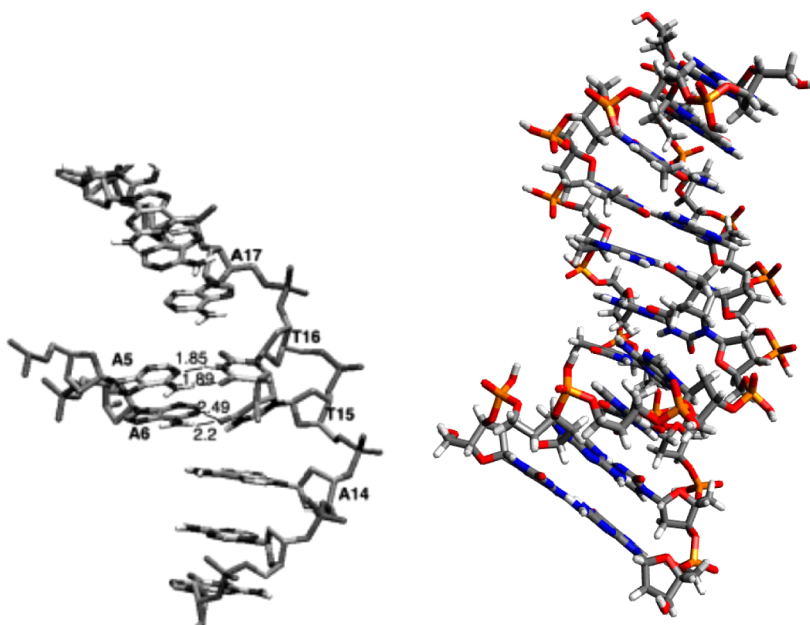


Figure 2. Two views of the 1N4E structure. On the left, the backbone kink near the $\text{T}_{15}=\text{T}_{16}$ damage site is emphasized and some of the nearby A bases are labeled. On the right, the base pairing and π -stacking and its disruption near the $\text{T}=\text{T}$ damage is emphasized. These views were constructed from data given in ref 35.

determined from the database. To obtain these distances, we replaced the base listed in the first column of Table 1 with an OG and measured distances between various atoms in the rings of OG to atoms in the rings and cyclobutane unit of T=T.

The distances labeled “minimum” in Table 1 were calculated as the shortest distance between an atom involved in the conjugated π orbitals of the OG unit replacing the base appearing in column 1 and an atom in the conjugated π orbitals of either ring of the T=T unit. These distances likely relate to the Coulomb interaction that arises when an electron is transferred from OG to T=T because this interaction will be dominated by contributions from π -orbital charge densities on the most proximal atoms. The distances labeled “middle” are measured between the midpoints of the T=T (i.e., at the center of the cyclobutane structure) and the OG replacing the base appearing in column 1.

The repair rates listed in the fifth column of Table 1 came from refs 1 and 10, and the quantum yield data in the sixth column came from ref 10. We will discuss these trends in repair rates and quantum yields in more detail in Section IIIC.

B. Energy and Dielectric Screening Considerations. As envisioned in ref 1 and summarized in Scheme 2, the OG-induced T=T repair process involves several steps: (i) Photoexcitation of an OG:X base pair that undergoes decay back to the ground state in competition with (ii) transfer of an electron from the excited OG*:X to the T=T to form the OG*:X...T=T⁻ ion pair, after which (iii) C-C bond cleavage within the T=T⁻ anion generates T and T⁻ in competition with (iv) back electron transfer from T=T⁻ to the OG⁺ cation prior to complete C-C bond cleavage, and, finally, (v) return electron transfer from T⁻ to OG⁺ after complete C-C bond rupture.

As discussed earlier, the competitions between steps iii and iv and between step ii and decay of photoexcited OG*:X play key roles in determining the efficiency of the T=T repair. For FADH⁻, step iii takes ~90 ps, whereas step iv takes 2400 ps, and the time it takes to transfer an electron to T=T (250 ps) is much less than the time it takes the excited FADH⁻ to decay (1300 ps). These rates allow FADH⁻ to have a T=T repair efficiency near unity.

Unfortunately, analogous ultrafast spectroscopy experiments have not yet been carried out for a system containing the OG:X...T=T unit. Nevertheless, as we attempt to demonstrate in this paper, we can combine a wide range of experimental findings to obtain reasonable estimates for most of the rate constants shown in Scheme 2 for the OG case. In arriving at such estimates, it is important to be aware of how these rates compare with the rate at which the surrounding solvent (mainly water) molecules can undergo dielectric relaxation because this determines whether the Coulomb interactions between the OG⁺:X and T=T⁻ ions will have a significant influence.

Free water molecules can reorient³⁶ to fully dielectrically screen ions in ~10 ps, whereas more tightly bound water molecules can take ~1000 ps to do so. After the initial photoexcitation of OG:X to form OG*:X, some solvent response will occur (because the OG*:X unit may have appreciable internal charge-transfer character), but not as much as after the electron moves from OG*:X to T=T to create the OG⁺:X T=T⁻ ion pair. It is generation of the latter charge-separated species that will induce the solvent to undergo major reorientation.

At the instant an ion pair is created, two responses of the surrounding medium (i.e., the solvent and the DNA frame-

work) take place. On a time scale of >10 ps, solvent reorientation that generates strong dielectric screening (e.g., consistent with dielectric constants near $\epsilon = 80$) occurs, but on a shorter time scale; only the electronic clouds of the surrounding medium have time to respond and do so in a manner that can be represented³⁷ by a dielectric constant near $\epsilon = 2$. So whether the Coulomb interaction between the OG⁺:X and T=T⁻ should be described as 14.4 eV Å/ ϵ R (Å) with $\epsilon = 2$ or $\epsilon = 80$ depends on how fast the electron is transferred to the T=T, how fast the C-C bond ruptures occur, and how fast the electron is transferred back to OG⁺:X to reform OG:X. If any of these steps requires considerably more than 10 ps, $\epsilon = 80$ is more appropriate; if any occurs within ~10 ps, $\epsilon = 2$ should be used.

Let us now consider the energy balances operative when 4.1 eV photons create OG⁺:X T=T⁻ ion pairs for dielectric environments characterized by ϵ values of 1, 2, and 80. We include the $\epsilon = 1$ (gas-phase) case only to emphasize the effects of solvation by contrasting its predictions with those of the $\epsilon = 2$ and $\epsilon = 80$ cases.

As noted earlier, the 4.1 eV photons used to excite the OG do not have enough energy to detach an electron from the OG molecule or from an OG:X base pair. However, the attractive Coulomb potential between an OG⁺:X and a T=T⁻ anion separated by a distance R lowers the energy of this ion pair state by 14.4 eVÅ/ ϵ R (Å), thus possibly bringing the photoexcited OG*:X...T=T system into energy resonance with the OG⁺:X...T=T⁻ state if the OG and T=T are within a critical distance, R*. These energy considerations are very different from what happens when an anionic donor such as FADH⁻ or LFH⁻ is used. For such systems, once a photon electronically excites the donor anion, it requires very little energy to extract an electron from the excited anion (i.e., the difference between the detachment energy of the anion and its electronic excitation energy is very small). In contrast, for OG, the electronic excitation energy (4.1 eV) is much smaller than the ionization energy (7.0 eV). So in the OG case, there has to be a source of ~2.9 eV to cause the electron to leave the excited OG*. In other words, the forward electron transfer step shown in Scheme 2 as being exothermic is actually endothermic for the OG case in the gas phase. However, there are at least two factors that act to stabilize the ion-pair state—solvation and Coulomb interaction—that can render the forward electron transfer exothermic, which we now explore in greater detail.

It is well established that the EAs of all of the isolated DNA bases are negative,³⁸ and we calculated the EA of the damaged T=T unit to be negative by 0.52 eV. Using 7.0 eV as the vertical³⁹ IP of OG:X and -0.52 eV as the EA of T=T and assuming a photon energy of 4.1 eV, the energy defect to forming the ion pair state is 3.4 eV. In the gas phase, to overcome this defect through an unscreened mutual Coulomb attraction, the OG⁺ and T=T⁻ ions would have to be within 4.2 Å. The minimum distances listed in Table 1 fall near or within this range for the A₁₄, A₁₇, T₄, and T₇ bases as well as for A₅ and A₆, but not for A₁₈ or A₁₃, although all eight produced measurable T=T repair. As explained earlier, we focus on the minimum distances because these distances relate best to how close an electron occupying a delocalized π LUMO of T=T can come to a hole (i.e., a missing electron) within a delocalized π HOMO of OG⁺:X, and it is the interaction between this electron and hole that constitute the Coulomb interaction. The middle distances relate to the center of the cyclobutane part of

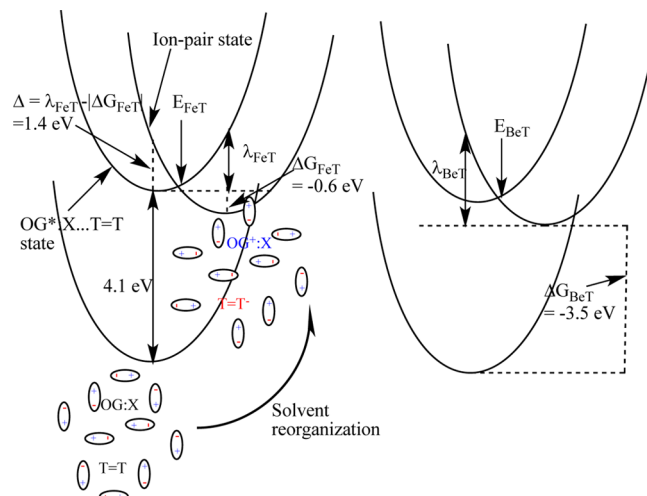
$T=T$, which is not where the electron initially resides in $T=T^-$.

The experiments are not carried out in the gas phase, however, so we need to examine instead how the energy-matching criterion would apply if electronic ($\epsilon = 2$) polarization or full static ($\epsilon = 80$) polarization were operative. We carried out ab initio calculations to compute the changes in the ionization potential of OG and the electron affinity of $T=T$ induced by dielectric polarization for ϵ values of 2 and 80. We found the IP of OG to reduce by 1 eV and the EA of $T=T$ to increase by 1 eV when the dielectric constant is changed from 1 to 2, whereas both were altered by ~ 2 eV if ϵ was changed from 1 to 80. These differential solvation values of 1 and 2 eV for each ion are in line with what the Born model's scaling formula ($1 - 1/\epsilon$) would suggest. These data tell us that to form a solvated $OG^+:X$ and a solvated $T=T^-$ requires an energy input of $7.0 - (1 \text{ or } 2) + 0.5 - (1 \text{ or } 2) \text{ eV} = 5.5 \text{ or } 3.5 \text{ eV}$, depending on whether ϵ is 2 or 80, respectively. In the $\epsilon = 80$ case, this means the 4.1 eV photons have more than enough energy to exothermically form the $OG^+:X \cdots T=T^-$ ion pair. However, for $\epsilon = 2$, the 4.1 eV photons alone do not possess enough energy; $5.5 - 4.1 = 1.4 \text{ eV}$ that needs to come from somewhere else to render ion-pair formation exothermic. We propose that, for processes occurring within $\sim 10 \text{ ps}$ of the formation of the ion-pair state, it is $\epsilon = 2$ Coulomb stabilization of the ion pair that can provide this 1.4 eV energy defect. Before discussing this issue further, we first think it appropriate to reflect on how the forward and back electron transfer steps are viewed in the conventional Marcus-theory framework. This allows us to make it clear how our proposal regarding Coulomb stabilization can contribute to the electron transfer processes in a manner that modifies but does not contradict the conventional framework.

Within the Marcus picture, even when exothermic as for $\epsilon = 80$, the electron transfer from $OG^*:X$ to $T=T$ or from $T=T^-$ back to $OG^*:X$ may have to surmount a barrier arising from the reorganization of the surrounding medium and of the internal bond lengths and angles of the $OG:X$ and $T=T$ moieties. In Figure 3, we show two sets of three parabolic energy surfaces depicting how the ground $OG:X \cdots T=T$, photoexcited $OG^*:X \cdots T=T$, and ion-pair $OG^+:X \cdots T=T^-$ states vary as functions of this phenomenological reorganization coordinate for the forward (left) and back (right) electron transfer events.

In the left portion of Figure 3 at the bottom, we attempt to emphasize how the surrounding medium (solvent) would have its dipoles more randomly oriented just prior to photon absorption (when in the $OG:X \cdots T=T$ state) as well as immediately after photon absorption (when in the $OG^*:X \cdots T=T$ state). In the left portion of Figure 3 near the middle, we show how the solvent's dipoles would exist when the system is in the $OG^+:X \cdots T=T^-$ ion-pair state once the solvent has had sufficient time to reorganize. It is important to emphasize that the ion-pair state's energy lies $\sim 1.4 \text{ eV}$ above that of $OG^*:X \cdots T=T$ if the solvent is not allowed to undergo full reorganization, absent the Coulomb stabilization that we discuss below.

To explain the origin of the numerical data shown in Figure 3, we remind the reader that, if the surrounding medium has enough time to fully reorganize, it is $\sim 0.6 \text{ eV}$ exothermic to move from $OG^*:X \cdots T=T$ to $OG^+:X \cdots T=T^-$. This value is obtained by taking the IP of OG (7 eV), lowering it to account for full solvation (-2 eV), subtracting the EA of $T=T$ (-0.5 eV), correcting for this anion's full solvation (-2 eV), and



$$\begin{aligned} E_{FeT} &= (\lambda_{FeT} - |\Delta G_{FeT}|)^2 / 4\lambda_{FeT} & E_{BeT} &= (\lambda_{BeT} - |\Delta G_{BeT}|)^2 / 4\lambda_{BeT} \\ \lambda_{FeT} &= \Delta + |\Delta G_{FeT}| & \lambda_{BeT} &= \Delta + |\Delta G_{BeT}| = \lambda_{FeT} \\ &= 2.0 \text{ eV} \end{aligned}$$

Figure 3. Schematic depiction of ground $OG:X \cdots T=T$ (bottom), excited $OG^*:X \cdots T=T$ (vertically above the ground), and $OG^+:X \cdots T=T^-$ ion-pair states and the Marcus theory reorganization energies λ and ΔG values associated with forward electron transfer (FeT; left) and back electron transfer (BeT; right). The horizontal axis characterizes the degree of reorganization of the surrounding medium ranging from that present soon after photon absorption (depicted near the bottom of the left figure) to when the medium has had time to fully rearrange to accommodate the charge-separation event (depicted near the middle of the left figure).

subtracting the energy of the photon (4.1 eV). However, as just explained, we know the $OG^+:X \cdots T=T^-$ electronic state lies vertically 1.4 eV above $OG^*:X \cdots T=T$. This is the energy we denote as Δ in Figure 3. These data mean that the reorganization energy for forward electron transfer is $\sim 2.0 \text{ eV}$, as shown in Figure 3, which in turn predicts a barrier of $\sim 0.25 \text{ eV}$ for the forward electron transfer if this event were to follow the traditional solvent fluctuation-induced pathway. For the back electron transfer process (see the right-hand part of Figure 3), we know that $\Delta G = -3.5 \text{ eV}$, and it can be shown, within the simple harmonic approximation used here, that the reorganization energy is the same as for forward electron transfer (2 eV), so the corresponding barrier is $\sim 0.28 \text{ eV}$. Because these estimates of the reorganization energies and exothermicities derive from our computed estimates of IPs, EAs, and solvation energies, they are probably not highly accurate.⁴⁰ Nevertheless, we offer them and the accompanying Figure 3 to introduce the discussion below about how Coulomb potentials are posited to alter the above mechanistic picture when the OG-to- $T=T$ distance is less than 5–6 Å, but not for longer distances.

The above analysis of the energy landscape ignores the stabilizing Coulombic interaction between the $OG^+:X$ and $T=T^-$ ions. In the region where $\epsilon = 2$ is applicable (when the solvent has not yet relaxed and thus for positions along the horizontal axis close to the minima in the ground and $OG^*:X \cdots T=T$ surfaces), this interaction can lower the energy of the ion-pair state by the amount labeled $\Delta = 1.4 \text{ eV}$ (or more) in Figure 3 if the two ions are within $R = 5–6 \text{ \AA}$.

Therefore, immediately after photon absorption and before full solvent reorganization occurs, the ion-pair state can actually lie *below* the OG^{*}:X···T=T state if R is less than 5–6 Å; for values of R beyond 6 Å, the ion-pair state remains above OG^{*}:X···T=T. This extra stabilization could be expected to enhance the rate of forward electron transfer for R values inside 5–6 Å because the forward electron transfer would not have to “wait” for thermal fluctuations to overcome the $E_{\text{FeT}} = 0.25$ eV barrier along the reorganization coordinate. Instead, a more vertical transition from OG^{*}:X···T=T to OG⁺:X···T=T⁻ could occur in an exothermic radiationless relaxation mechanism (i.e., an internal conversion similar to what is widely believed⁴¹ to contribute to the short lifetimes of nucleobases) that would not require the solvent to fully relax. It is this kind of effect that we posit might contribute to making the OG-induced T=T repair different from the FADH⁻ case, in particular by enhancing forward electron transfer whenever the ion-pair separation is less than 5–6 Å.

In our opinion, the limited spatial range of repair observed in ref 1 and summarized in Table 1 seems to be in line with this suggestion (i.e., A₁₇, A₁₄, A₁₈, A₁₃, T₁₈, T₁₃, A₅, and A₆ all have minimum distances within or very near 5–6 Å, and no T=T repair was observed when OG was placed farther away). Of course, these data do not prove that our proposition is correct, so more experimental studies as outlined later would be helpful to test this hypothesis.

The above analysis shows that it is energetically possible to form the OG⁺:X···T=T⁻ ion pair using 4.1 eV photons to excite OG:X···T=T either by having solvent reorganization control the forward electron transfer rate (i.e., by moving over the barrier of height E_{FeT}) or by Coulomb stabilization lowering the ion-pair state’s energy. Moreover, it explains why we propose that ion-pair distances limited to 5–6 Å might play a role in accelerating forward electron transfer. However, we still need more information to put limits on k_{FeT} , k_{LT} , k_{BC} , and k_{BeT} for the OG case, and it is to this end that we now turn our attention.

C. Components of the T=T Repair Rates and How They Might Depend on Interbase Distances. As mentioned earlier, the Burrows group recently determined¹⁰ the quantum yields for T=T repair (i.e., percent of absorbed photons that generate T=T repair) for a variety of sequences similar to those shown in Figure 1. We list these quantum yields in the rightmost column of Table 1. Two observations are important to make regarding these data. First, the fact that all the quantum yields are 1% or less tells us that either (i) k_{BeT} is ~100 times k_{BC} while k_{FeT} is much larger than k_{LT} , (ii) k_{FeT} is ~1% of k_{LT} while k_{BeT} is considerably smaller than k_{BC} , or (iii) the truth is somewhere between these two limits (e.g., k_{FeT} could be 10% of k_{LT} while k_{BeT} is 10 times k_{BC}). Second, the fact that the ratios of these quantum yields appears to track the ratios of repair rates suggests that it is the probability of an electron’s being transferred from OG^{*}:X to T=T that governs the relative repair rates among these sequences rather than, for example, differences in back electron transfer rates or rates of C–C bond cleavage.

Two more experimental facts can be used to further refine our estimates for the relative values of k_{LT} and k_{FeT} . First, Schwalb et al.⁴² determined the fluorescence lifetime of excited Watson–Crick paired G:C to be 0.355 ps. Later, de La Harpe et al.⁴³ examined the effects of base π-stacking on these G:C lifetimes, and both groups concluded that proton-coupled electron transfer (PCET) accelerates the rate of decay of the

excited G:C. In a nice review, Kumar and Sevilla⁴⁴ explained how this rate acceleration occurs in terms of a conical intersection model.⁴⁵ The second set of data comes from the Burrows lab,¹⁰ where they measured the T=T repair rates for sequences equivalent to those labeled A₁₇, A₁₄, A₁₈, and A₁₃ in Table 1 but with the OG base paired not with an A but with a C. The repair rates found for these four sequences were⁴⁶ 1.1, 0.4, 0, and 0×10^{-2} min⁻¹, respectively, compared with the rates of 3, 1.5, <0.2, and 0.2×10^{-2} min⁻¹ listed in Table 1 for the corresponding sequences when OG is paired with A.

Assuming, as in ref 1, that pairing OG with C rather than with A causes Burrows’ observed reduction in T=T repair by a factor of ~3 by making OG:C’s lifetime ($1/k_{\text{LT}}$) ~3 times shorter than OG:A (i.e., with the PCET being operative in OG:C but not in OG:A), we conclude that k_{LT} is larger than k_{FeT} . The fraction of excited OG^{*}:X that undergo forward electron transfer ($k_{\text{FeT}}/(k_{\text{FeT}} + k_{\text{LT}})$) would not be so strongly decreased by increasing k_{LT} if k_{FeT} were greater than k_{LT} . So, we know that $k_{\text{FeT}} < k_{\text{LT}}$, but we also know that k_{FeT} must be at least as large as 0.01 k_{LT} ; otherwise, the repair quantum yields would not be 1%, as they are found to be. If we assume that the lifetime of OG^{*}:C is close to that measured in ref 42 for G^{*}:C (0.355 ps) and that the lifetime of OG^{*}:A is three times longer, this would suggest that $0.01 \text{ ps}^{-1} < k_{\text{FeT}} < 1 \text{ ps}^{-1}$. Even without assuming OG^{*}:A has a lifetime near 1 ps, we know that $0.01k_{\text{LT}} < k_{\text{FeT}} < k_{\text{LT}}$.

We still need more information to reach conclusions about k_{BeT} and k_{BC} , and it is to obtain a reasonable estimate of k_{BC} that we analyze our ab initio data in Sections IIID and IIIE. To then estimate k_{BeT} , we make use of trends in experimental data from Takaya et al.⁴⁷ However, before addressing what happens after T=T⁻ is formed, let us reflect a bit more on the relative T=T repair rates among the sequences described in Table 1.

The proposed involvement of Coulomb short-time stabilization provides one possible rationalization for why the range of T=T repair is limited to 5–6 Å, but we still need to explain how the relative rates of repair can be related to the OG-to-T=T distances. It is possible that distance variations in the rates of back electron transfer from T=T⁻ to OG⁺:X could govern the overall repair rates. However, one would expect these back transfer rates to be fastest and, thus, the repair rate lowest when the ion-pair distance is smallest, which is not what the data in Table 1 show. Alternatively, it could be that the rate of C–C bond cleavage within the T=T⁻ anion could depend on the distance to the OG^{*}:X. However, this is not the case, as we illustrate in Section IIIE. The third possibility is that, as we suggested earlier, the net rate of repair is governed by the rate at which electrons arrive at the T=T site from the excited OG^{*}:X. It is this latter case that we now focus on.

In Table 1, we show in column 4 we show values of $3e^{-\beta(R_{\text{middle}} - 5.4\text{\AA})}$ with a value of $\beta = 0.6 \text{ \AA}^{-1}$ to test to what extent the T=T repair rates shown in column 5 appear to decay exponentially with distance. A factor of 3 is used to link the value in column 4 for the sequence (A₁₄) having the highest repair rate to the rate reported in column 5. The specific decay parameter (0.6 \AA^{-1}) was found to provide a good fit to the observed repair rates. Although not quantitative, the values of $3e^{-\beta(R_{\text{middle}} - 5.4\text{\AA})}$ do seem to track the repair rates, especially for sequences (A₁₇, T₄, T₇), for which one expects direct spatial overlap of the OG^{*} and T=T π* orbitals. For sequences (A₁₈, A₁₃) that have an intervening base between the OG^{*} and T=T, the $3e^{-\beta(R_{\text{middle}} - 5.4\text{\AA})}$ ratios are also in reasonable (but not as

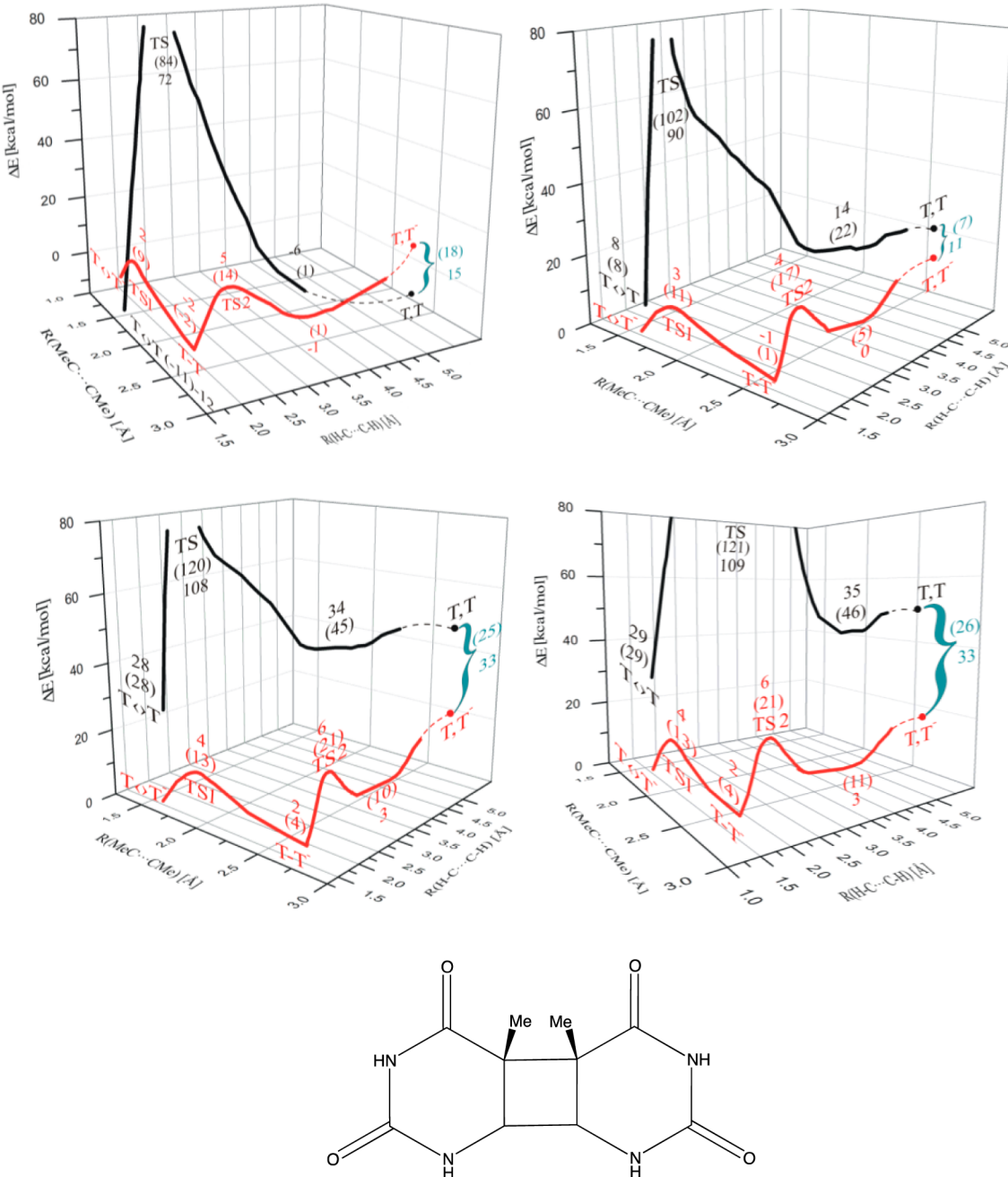


Figure 4. Energy profiles for opening of the cyclobutane-like ring in neutral $T=T$ (black) and anionic $T=T^-$ (red) evaluated in environments corresponding to dielectric constants of 1, 2, 37, and 80 (upper left, upper right, lower left, lower right, respectively). Also shown is the local bonding structure of the $T=T$ unit with its cyclobutane feature in the center. The energy of the $T=T^-$ anion is defined as zero in all cases. MP2-level energies are shown without parentheses, and HF-level energies are shown in parentheses.

good as for A_{17} , T_4 , T_7) agreement with the observed repair rates.

The A_5 and A_6 data do not appear to be tracked well by the $3e^{-\beta(R_{\text{middle}}-5.4\text{\AA})}$ fit. For A_5 , the observed repair rate is double what the fit predicts, and for A_6 , it is $\sim 25\%$ of the fit's prediction, even though both sequences have similar R_{middle} values. This suggests that, when in the strand opposite from the $T=T$ and located directly opposite the $T=T$, some factor other than that reflected in $3e^{-\beta(R_{\text{middle}}-5.4\text{\AA})}$ is operative.

It is appropriate to point out that the exponential decay parameter ($\beta \approx 0.6 \text{ \AA}^{-1}$) used in the $3e^{-\beta(R_{\text{middle}}-5.4\text{\AA})}$ expression falls within the range characteristic of superexchange type electron transfer events well-known⁴⁸ to occur in DNA. The

fact that the variations in repair rates among the sequences studied in ref 1 appear to be tracked using the $3e^{-\beta(R_{\text{middle}}-5.4\text{\AA})}$ formula suggests that the rate at which electrons arrive at the $T=T$ is what governs the repair rates. The exceptions (A_5 , A_6) tell us that there is more to the story that we still need to explore.

D. Why We Need To Examine the Reaction Potential Energy Landscape. Even if the model introduced above rationalizes how (via the Coulomb ion-pair energy overcoming the energy defect) and at what relative rates (determined by the flux of electrons leaving OG* that strike the $T=T$ site) the repair might occur, it still remains to explain what happens after an electron has attached to $T=T$ to form the $T=T^-$ unit

because it may well be that energy barriers on the reaction surface connecting $T=T^-$ to $T + T^-$ are really what governs the relative repair rates listed in Table 1. As we discussed earlier, the most recent theoretical and experimental studies^{16–21} suggest that the evolution of the anionic $T=T^-$ energy surface passes over very small barriers and results in cleaving both of the cyclobutane unit's C–C bonds within tens to hundreds of picoseconds. However, none of those studies involved a proximal positively charged group, such as our $OG^+ \cdot X$ cation. For this reason, we decided to perform our own ab initio study of the $T=T^-$ anion's energy landscape when an OG^+ is at a distance representative of the cases shown in Table 1 for which $T=T$ repair was observed. We needed to determine whether the presence of the OG^+ group would qualitatively alter the energy landscape, which could be expected if, during the evolution from $T=T^-$ to $T + T^-$, the anion's charge distribution moved significantly away from or toward the proximal OG^+ .

It is well-known that the [2 + 2] cycloaddition reaction that formed the two C–C σ bonds holding the thymine units together has a large symmetry-imposed barrier on its ground-state energy surface. It is also known that photoexciting one of the thymine molecules removes the symmetry constraints on the [2 + 2] cycloaddition reaction and causes the reaction to occur at a fast rate on the excited-state energy surface. Neither of these cases pertains to the bond cleaving in the $T=T^-$ anion, where an excess electron initially occupies a π^* orbital on the thymine dimer. Cederbaum and co-workers⁴⁹ recently studied the electron-induced cleavage of the cyclobutane unit within quadricyclanone to form norbornadieneone in which the carbonyl unit's π^* orbital is where the electron was initially bound. They used Woodward–Hoffmann analysis to explain how such reactions become “allowed” when there is one excess electron, and we think their analysis is applicable to our case, as well. Other workers^{50–53} examined the possibility that electron transfer from or to $T=T$ (or similar photodamaged species) could induce repair. These studies and more recent modern theoretical studies^{16–18,21} all show that the bond cleaving reaction on the anion surface is, indeed, quite facile and unhindered by large energy barriers. However, none of these studies involved a proximal positively charged group, which might be expected to alter the energy landscape.

E. The $T=T^-$ Anion's Energy Surface without and with a Proximal OG^+ . In Figure 4, we display the energies (at the HF and MP2 levels) of the neutral and anionic $T=T$ species as functions of two coordinates: (i) the C–C distance within the cyclobutane unit relating to the two carbon atoms having attached methyl groups and (ii) the C–C distance between the other two carbon atoms in the cyclobutane unit. As these two coordinates are extended, the cyclobutane ring is broken. The paths traced in Figure 4 lie on IRC paths, so they properly connect local minima through true transition states.

For the anion case, we searched for a reaction path and corresponding transition state in which both of these bonds break in a concerted manner, but we found the lowest-energy path to be the sequential two-step path characterized in Figure 4. For the neutral species, we identified a concerted reaction path connecting $T=T$ to the two thymine fragments. These two paths are described by the red (anion, sequential) and black (neutral, concerted) curves in Figure 4, respectively.

There are several features of the four energy profiles shown in Figure 4 that are important to note:

- 1 For the nonsolvated case, the $T=T^-$ starting material and the $T + T^-$ products are electronically unstable with respect to their neutral counterparts by 12 and 15 kcal mol⁻¹, respectively. However, with even weak solvation (e.g., a dielectric constant of 2), these anionic species become electronically stable (and more so with stronger solvation).
- 2 As expected, the neutral energy surfaces have very large (symmetry-imposed) barriers along the concerted ring-opening reaction path. These large barriers persist, regardless of the degree of solvation.
- 3 In the sequential reaction path associated with the anionic reaction, to break the first C–C bond (the $C_5-C_{5'}$ bond) in the cyclobutane unit of $T=T^-$ requires surmounting a very small barrier (2, 3, or 4 kcal mol⁻¹ for $\epsilon = 1, 2$, or 80, respectively). After corrections for zero-point energy differences (-2 kcal mol⁻¹) and after adding in entropic contributions ($-T\Delta S = -0.3$ kcal mol⁻¹), these barriers reduce to 0, 0.7, or 1.7 kcal mol⁻¹, respectively. Assuming a pre-exponential factor of 10^{13} s⁻¹, even a 1.7 kcal mol⁻¹ barrier could be surmounted in a few picoseconds.
- 4 After breaking the first C–C bond, an intermediate (in which the excess electron resides on one of the methylated carbon atoms) is formed whose energy lies within 1–2 kcal mol⁻¹ below that of the $T=T^-$ starting material. Solvation appears to have little influence over the energy of this intermediate relative to $T=T^-$.
- 5 To move from the intermediate just discussed and cleave the second C–C bond requires surmounting a barrier with size of 7, 5, or 4 kcal mol⁻¹ for $\epsilon = 1, 2$, or 80, respectively. After corrections for zero-point energy (-2 kcal mol⁻¹) differences and after adding in entropic contributions ($-T\Delta S = -0.5$ kcal mol⁻¹), these barriers reduce to 4.5, 2.5, or 1.5 kcal mol⁻¹, respectively.
- 6 The two-step ring-opening reaction (from $T=T^-$ to form neutral T and T^- anion weakly bound by their intermolecular forces) has a $\Delta E_{\text{reaction}}$ between -1 and $+3$ kcal mol⁻¹, depending on the solvation environment. In other words, the overall reaction is nearly thermoneutral, and its thermochemistry is not affected much by solvation.

These findings are very much in line with what earlier workers have found: small barriers for $C_5-C_{5'}$ and $C_6-C_{6'}$ cleavage that are easily surmounted at room temperature. Although we still need to ascertain the effect of the OG^+ ion's charge on these barriers, these data suggest that, as in photolyase, it should take no more than ~ 100 ps for both C–C bonds to be cleaved. However, during this time frame, there can be considerable relaxation of the surrounding water molecules, so it is appropriate to use the $\epsilon = 80$ data when viewing the $T=T^-$ -to- $T-T^-$ -to- $T + T^-$ landscape.

As mentioned earlier, we also carried out calculations on a model system containing both the OG and $T=T$ units, doing so at geometries representative of $OG^+ \cdots T=T^-$, $OG^+ \cdots T-T^-$, and $OG^+ \cdots T \cdots T^-$ and of the transition states connecting these stationary points. The model systems, representative of the A_{17} and A_{14} cases in Table 1, are shown in Figure 5, in particular at geometries describing the system prior to electron transfer.

In Figures 6 and 7, we show the singly occupied molecular orbitals (one localized on the OG^+ , one on the $T=T^-$) for geometries associated with the transition state, over which the

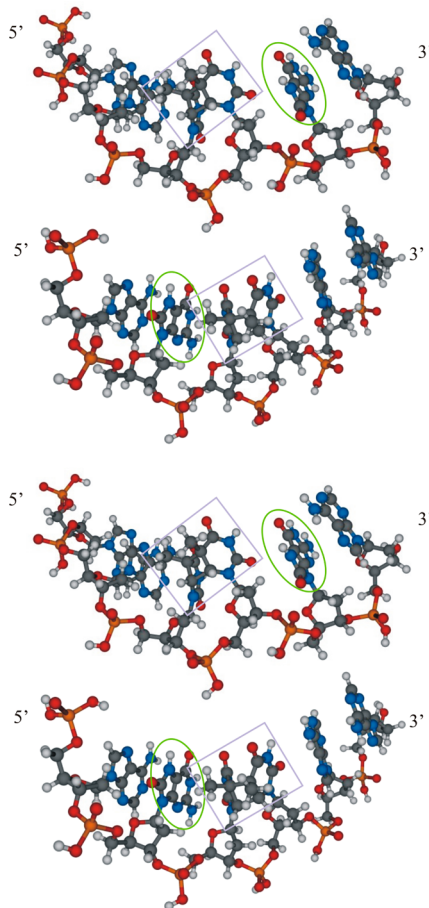


Figure 5. Structures of the model systems at geometries prior to electron injection. At the top is shown the structure in which OG (green circle) replaces A₁₇; at the bottom, the structure in which OG replaces A₁₄ is shown. The T=T damage unit is indicated by the blue square.

C₅–C_{5'} bond in the cyclobutane is cleaved (Figure 6) and with the transition state over which the C₆–C_{6'} bond is broken (Figure 7).

The value in displaying these orbitals lies in the fact that they provide convincing evidence that the electronic state we are probing indeed has OG⁺···T=T⁻ character and is not a state in which only the OG is excited (i.e., evidence that our calculation did not undergo variational collapse to the ground OG···T=T state).

We also computed the two barriers connecting OG⁺···T=T⁻ to OG⁺···T-T⁻ and OG⁺···T-T⁻ to OG⁺···T···T⁻ within this ONIOM-based study, and we did so for dielectric constants of 1 and 2. Because the geometries of the thymine dimer unit we used to carry out these calculations were determined for the isolated thymine dimer anion as described earlier, they cannot be assumed to be precise minimum or transition-state geometries for the OG⁺···T=T⁻ system. It was not computationally feasible to reoptimize the geometries for the full OG⁺···T=T⁻ system. As a result, the barriers that we obtained, which are shown in Table 2, are probably not as accurate as those shown earlier in Figure 4, but recall that our main reason for performing the OG⁺···T=T⁻ calculations was to see if the presence of the positive charge produced substantial alterations in the energy landscape.

Recall that these are electronic energy barriers that need to be corrected for zero-point energy differences and for entropic effects. After doing so, the first barrier drops to 0.7 kcal mol⁻¹, and the second reduces to 4.5 kcal mol⁻¹ for $\epsilon = 1$ and 3.5 kcal mol⁻¹ for $\epsilon = 2$.

The most important conclusion to be drawn from our study of the reaction energy profile for OG⁺···T=T⁻ case in comparison with our findings for the T=T⁻ system that is absent OG⁺ is that the presence of the proximal positively charged OG⁺ does not have a major influence on the barriers that T=T⁻ must surmount to evolve into T-T⁻ and then into T + T⁻. This suggests that, once the electron resides on the T=T fragment, the rates of cleavage of the C₅–C_{5'} and C₆–C_{6'} bonds in OG⁺···T=T⁻ should be expected to be similar to those in the FADH⁻ or LFH⁻ cases. At most, there may be a 1 kcal mol⁻¹ increase in the second barrier when the OG⁺ cation is present. Therefore, we have every reason to believe that both C–C bonds are cleaved within a few hundred picoseconds in

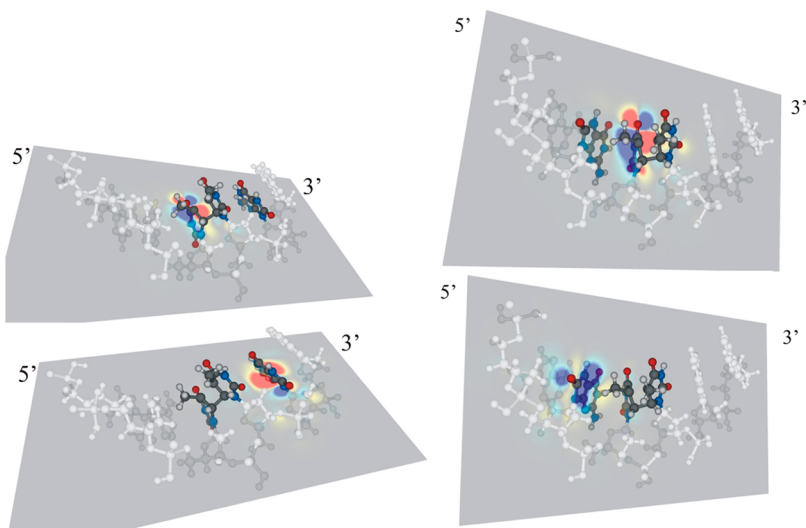


Figure 6. Singly occupied orbitals of T=T⁻ and of OG⁺ at the transition state associated with cleaving the first C–C bond in the cyclobutane unit when OG replaces A₁₇ (left) and when OG replaces A₁₄ (right).

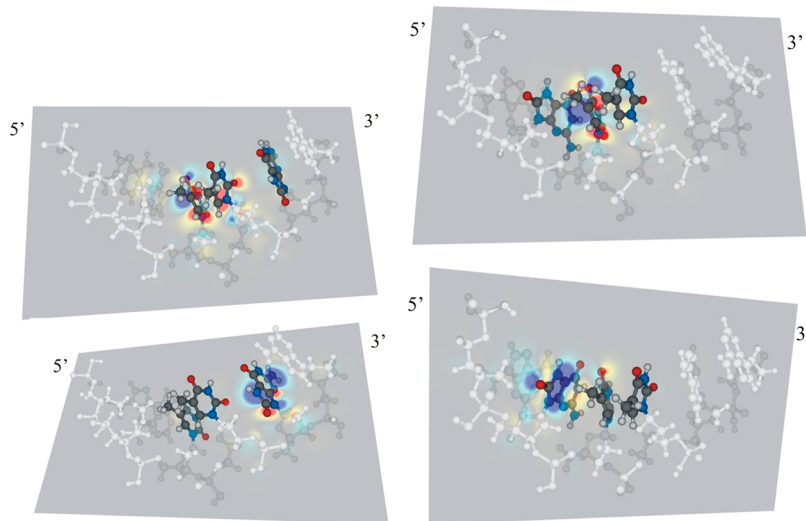


Figure 7. Singly occupied orbitals of $T=T^-$ (top) and of OG^+ (bottom) at the transition state associated with cleaving the second C–C bond in the cyclobutane unit when OG replaces A_{17} (left) and when OG replaces A_{14} (right).

Table 2. Barriers Connecting $OG^+\cdots T=T^-$ to $OG^+\cdots T-T^-$ and $OG^+\cdots T-T^-$ to $OG^+\cdots T\cdots T^-$ for the A_{14} Case at Two Values of the Dielectric Constant

base replaced by OG	first barrier kcal mol ⁻¹ ; $\epsilon = 1$	second barrier kcal mol ⁻¹ ; $\epsilon = 1$	first barrier kcal mol ⁻¹ ; $\epsilon = 2$	second barrier kcal mol ⁻¹ ; $\epsilon = 2$
A_{14}	3	7	3	6

the $OG^+\cdots T=T^-$ case, which is similar to the rate for the photolyase- and LFH⁻-containing systems.

Recall that we earlier were able to place limits on the relative sizes of k_{LT} and k_{FeT} : $0.01 k_{LT} < k_{FeT} < k_{LT}$. If k_{FeT} were nearly equal to k_{LT} , k_{BeT} would have to be ~ 100 times k_{BC} (i.e., $k_{BeT} \approx 1 \text{ ps}^{-1}$) to be consistent with the observed $\sim 1\%$ $T=T$ repair quantum yield. If k_{FeT} were only 1% of k_{LT} , k_{BeT} would have to be comparable to or less than k_{BC} (i.e., $k_{BeT} \approx 0.01 \text{ ps}^{-1}$ or less). Of course, other combinations also exist that are compatible with the 1% repair yield. For example, k_{FeT} could be 10% of k_{LT} and k_{BeT} could be 10 times k_{BC} .

To further refine our estimates, we turn to data summarized in Figure 4 of ref 47, where we see a near-linear plot of the decay rates of dinucleosides vs the gas-phase IP-EA values of the two bases appearing in the dinucleoside (the authors note that the linear relation is also obtained if one uses the solution-phase redox potentials of the two bases). If we assume this correlation applies to the case at hand with $OG:X$ being the electron donor and $T=T$ the electron acceptor, $IP = 7 \text{ eV}$ and $EA = -0.5 \text{ eV}$, so $IP-EA = 7.5 \text{ eV}$. Using this value of IP-EA in the linear plot of Figure 4 in ref 47 produces a value for $k_{BeT} \approx 0.1 \text{ ps}^{-1}$.

Returning to the estimates made in the preceding paragraphs and now assuming that $k_{BeT} \approx 0.1 \text{ ps}^{-1}$ and $k_{BC} \approx 0.01 \text{ ps}^{-1}$, we can conclude that k_{FeT} must be $\sim 10\%$ of k_{LT} for the $OG:X\cdots T=T$ system under discussion. If we could assume that k_{LT} were approximately one-third that measured for $G^*:C$ (i.e., 1 ps^{-1}), we could predict that k_{FeT} is $\sim 0.1 \text{ ps}^{-1}$. These rate ratios suggest that $\sim 10\%$ of the initially excited $OG^*:X$ species transfer an electron to $T=T$ and that $\sim 10\%$ of the $T=T^-$ anions thus formed survive through the bond-cleavage steps (90% undergo back electron transfer). Clearly, these predictions should be amenable to experimental testing if

systems similar to the duplexes studied in ref 1 were subjected to ultrafast spectroscopic probes.

IV. DISCUSSION

We can now put forth our suggestion about how the full OG^* -induced $T=T$ repair process might be taking place for the species studied in ref 1, as outlined in Scheme 2:

Step 1 A photon with energy near 4.1 eV is absorbed by OG (within an $OG:X$ pair) to generate the electronically excited $OG^*:X$ species that is separated from the $T=T$ unit by a distance dictated by the internal bonding of the damaged sequence. Because excited states of A, T, G, and C lie higher than 4.1 eV, transfer of the electronic excitation of OG^* to any of these bases cannot occur, so the excitation remains localized on the $OG^*:X$. $T=T$ also has no excited states in this energy range, so formation of electronically excited $T=T$ can also be ruled out. The electronically excited $OG^*:X$ can decay to its ground state with a rate k_{LT} (that we estimate as 1 ps^{-1} , but experimental determination of this rate is much needed).

Step 2 If the OG^* and $T=T$ units have their minimum distances less than $\approx 5-6 \text{ \AA}$, the $OG^*\cdots T=T$ energy lies above that of $OG^+\cdots T=T^-$ prior to any but electronic cloud reorganization of the surrounding. This makes it exothermic for an electron to transfer from $OG^*:X$ to $T=T$ to form the ion pair via a radiationless relaxation in which the energy release is converted from electronic into vibrational energy. Experiments in which k_{LT} is increased by pairing OG with C rather than with A show reductions in $T=T$ repair rates. This tells us that k_{LT} exceeds k_{FeT} , and the observed $T=T$ repair quantum yield of 1% tells us that k_{LT} cannot exceed k_{FeT} by more than a factor of 100. Combining this information with our estimates of k_{BeT} and k_{BC} , we estimate k_{FeT} to be $\sim 10\%$ of k_{LT} (i.e., 0.1 ps^{-1} if our estimate of $k_{LT} \approx 1 \text{ ps}^{-1}$ is valid). If the OG^* -to- $T=T$ distance exceeds $5-6 \text{ \AA}$, it is still exothermic to transfer an electron from $OG^*:X$ to $T=T$, but this process must proceed through the conventional solvent-fluctuation-activated pathway that is presumably slow

enough not to generate detectable T=T repair in the experiments of ref 1. The limited spatial extent over which T=T repair is observed supports this interpretation.

Step 3 Once on the OG⁺:X···T=T⁻ ion-pair energy surface, a very small barrier (see Figure 4) can be surmounted to generate the intermediate OG⁺···T-T⁻ ion pair in which one C-C bond of the cyclobutane has cleaved. Subsequently, a somewhat higher, albeit still small, barrier can be surmounted to cleave the second C-C bond and generate an intact thymine and a thymine anion. Both of these bonds are cleaved within ~100 ps ($k_{BC} \approx 0.01 \text{ ps}^{-1}$), after which the excess electron can return from the nascent T⁻ to the OG⁺:X to form OG:X and two intact thymine units and complete the catalytic cycle.

Step 3' During the ~100 ps it takes for T=T⁻ to evolve through T-T⁻ and into T + T⁻, back electron transfer to the OG⁺:X takes place at a rate of $\sim k_{BeT} \approx 0.1 \text{ ps}^{-1}$. Because this back electron transfer takes less time than for the surrounding solvent to fully relax, the partially screened Coulomb potential 14.4 eV Å/2R (Å) remains operative and may also facilitate the electron transfer from T=T⁻ to OG⁺:X. The competitions between step 2 and the lifetime and between step 3' and step 3 limit the efficiency of T=T repair to 1%, which is quite different from the photolyase case, which has an efficiency near 100%.

IV. CONCLUSIONS

A wide variety of experimental data, as well as basic considerations of DNA sequence geometry, time scales, and electrostatics were employed in an attempt to interpret the thymine dimer repair rate data found in experiments of ref 1. Ab initio electronic structure calculations were used to exclude that possibility that the proximal charged OG⁺:X unit would alter the energy landscape for T=T⁻ undergoing C-C bond cleavage. Having established that this is not the case, we could make use of results from earlier workers who probed theoretically and experimentally the C-C bond cleavage rates in systems not possessing a nearby charged unit.

Our studies support a picture within which the T=T repair process involves (1) electronic excitation of the OG:X unit within the duplex to form OG^{*}:X, which decays at a rate of k_{LT} (estimated to be ~1 ps⁻¹) in competition with (2) forward transfer of an electron from the excited OG^{*}:X to the T=T site. We propose that this process is rendered exothermic even in the absence of full solvent relaxation by the partially screened attractive Coulomb potential between the nascent OG⁺:X cation and T=T⁻ anion but only if the T=T and OG units are closer than ~5–6 Å. This forward electron transfer is estimated to occur at a rate 10% that of k_{LT} (i.e., $k_{FeT} \approx 0.1 \text{ ps}^{-1}$). For OG-to-T=T distances beyond 5–6 Å, forward electron transfer may still occur via a solvent-fluctuation activated process, but probably at a rate too slow to yield measurable T=T repair under the conditions used in ref 1. (3) Once a T=T⁻ anion is formed, subsequent reaction on the anion's potential energy surface proceeds through two low-energy barriers connecting T=T⁻ to the intermediate T-T⁻ and finally to T···T⁻, in which the cyclobutane unit is fully broken and two intact thymine sites are reestablished. This reaction takes ~100 ps (i.e., $k_{BC} \approx 0.01 \text{ ps}^{-1}$), which is comparable to

what has been found in the photolyase case. (4) During the T=T⁻ to T···T⁻ reaction, a competitive process in which back electron transfer from T=T⁻ to the OG⁺:X cation is estimated to take place at a rate ~10 times the rate of C-C bond cleavage (i.e., $k_{BeT} \approx 0.1 \text{ ps}^{-1}$). (5) Competition between back electron transfer and bond cleavage in combination with competition between lifetime decay and forward electron transfer limits the quantum yield of T=T repair to ~1%. In contrast, the back electron transfer rates in photolyase are much slower (2400 ps) and the lifetime is much longer (1500 ps), as a result of which the T=T repair efficiency approaches 100%. (6) The relative rates of T=T repair among the series of sequences studied in ref 1 correlate with an exponential decay distance dependence having a decay parameter $\beta \approx 0.6 \text{ \AA}^{-1}$. This suggests that variations in the rates at which electrons arrive at the T=T are what cause variations in the T=T repair rates among the various sequences.

Clearly, experimental data on the decay lifetime of OG^{*}:X would shed much light on the predictions made here. It would also be very useful to experimentally probe (e.g., using ultrafast spectroscopic means) the growth and subsequent decay of the T=T⁻ species; this would provide crucial information about k_{FeT} and $k_{BC} + k_{BeT}$. We hope that the analysis and predictions offered here will encourage experimental workers to undertake such studies.

■ AUTHOR INFORMATION

Corresponding Author

*E-mail: simons@chem.utah.edu.

Notes

The authors declare no competing financial interest.

■ ACKNOWLEDGMENTS

J.S. acknowledges several helpful conversations with Prof. C. J. Burrows and her student K. Nguyen. This work has been supported by NSF Grant No. 0806160 to J.S. and NCN Grant No. DS/8371-4-0137-12 to P.S. Computer resources from the Center for High Performance Computing at the University of Utah and from the Academic Computer Center in Gdańsk (TASK) are also acknowledged. This paper is dedicated to our friend and colleague, Peter Armentrout, a great science collaborator.

■ REFERENCES

- (1) Nguyen, K. V.; Burrows, C. J. *J. Am. Chem. Soc.* **2011**, *133*, 14586–14589.
- (2) Chinnapan, D. J. F.; Sen, D. *Proc. Natl. Acad. Sci.* **2004**, *101*, 65–69.
- (3) Sancar, A. *Chem. Rev.* **2003**, *103*, 2203–2237.
- (4) Carell, T.; Burgdorf, L. T.; Kundu, L. M.; Cichon, M. *Curr. Opin. Chem. Biol.* **2001**, *5*, 491–499.
- (5) Friedberg, E. C. *Nature* **2003**, *421*, 436–440.
- (6) OG^{*}:X may, for example, be a $^1\pi\pi^*$ state that could relax very quickly to another state of very similar energy, which actually transfers the electron to the T=T. For simplicity, we will use the symbol OG^{*}:X to denote both the originally photoexcited state and the state transferring the electron. In this case, k_{LT} is the rate constant determining the lifetime for returning OG^{*}:X to its ground electronic state.
- (7) As we discuss later, there are two separate C-C bond cleavage events. In Scheme 2, we represent the combination of these two cleavages as one event that has a rate constant k_{BC} .
- (8) Liu, Z.; Tan, C.; Guo, X.; Kao, Y-T.; Li, J.; Wang, L.; Sancar, A.; Zhong, D. *Proc. Natl. Acad. Sci.* **2011**, *108*, 14831–14836.

- (9) Kao, Y.-T.; Song, Q-H; Saxena, C.; Wang, L.; Zhong, D. *J. Am. Chem. Soc.* **2012**, *134*, 1501–1503.
- (10) Personal communication from Prof. C. J. Burrows to J.S.
- (11) Pacheco-Ortin, S.; Lozano, R. G.; Valdes, E. A. *Int. J. Quantum Chem.* **2012**, DOI: 10.1002/qua.24001 (online; print not yet available). This reference reported a value of 7.9 eV for the vertical IP; we computed the vertical IP to be 7.7 eV (at the MP2 level) to 8.1 eV (from an OVGF calculation).
- (12) Crespo-Hernandez, C. E.; Arce, R.; Ishikawa, Y.; Gorb, L.; Leszczynski, J.; Close, D. M. *J. Phys. Chem. A* **2004**, *108*, 6373–6377.
- (13) Pluharova, E.; Jungwirth, P.; Bradforth, S. E.; Slavicek, P. *J. Phys. Chem. B* **2011**, *115*, 1294–1305.
- (14) Reynisson, J.; Steenken, S. *J. Mol. Struct.: THEOCHEM* **2005**, *723*, 29–36.
- (15) Holman, M. R.; Ito, T.; Rokita, S. E. *J. Am. Chem. Soc.* **2007**, *129*, 6–7.
- (16) Hassanali, A. A.; Zhong, D.; Singer, S. *J. J. Phys. Chem. B* **2011**, *115*, 3848–3859.
- (17) Hassanali, A. A.; Zhong, D.; Singer, S. *J. J. Phys. Chem. B* **2011**, *115*, 3860–3871.
- (18) Masson, F.; Laino, T.; Tavernelli, I.; Rothlisberger, U.; Hutter, J. *J. Am. Chem. Soc.* **2008**, *130*, 3443–3450.
- (19) These authors cite much earlier work for explaining this effect: Hartman, R. F.; Van Camp, J. R.; Rose, S. D. *J. Org. Chem.* **1987**, *52*, 2684–2689. and Heelis, P. F. *J. Mol. Model.* **1995**, *1*, 18–21.
- (20) Chatgilialoglu, C.; Guerra, M.; Kaloudis, P.; Houee-Levin, C.; Marignier, J-L; Swaminathan, V. N.; Carell, T. *Chem.—Eur. J.* **2007**, *13*, 8979–8984.
- (21) Anthony, J.; Medvedev, D. M.; Stuchebrukhov, A. A. *J. Am. Chem. Soc.* **2000**, *122*, 1057–1065.
- (22) Pan, Z.; Chen, J.; Schreier, W.; Kohler, B.; Lewis, F. D. *J. Phys. Chem. B* **2012**, *116*, 698–704.
- (23) McLean, A. D.; Chandler, G. S. *J. Chem. Phys.* **1980**, *72*, 5639–5648.
- (24) Krishnan, R.; Binkley, J. S.; Seeger, R.; Pople, J. A. *J. Chem. Phys.* **1980**, *72*, 650–654.
- (25) Gonzales, C.; Schlegel, H. B. *J. Chem. Phys.* **1989**, *90*, 2154–2161.
- (26) Gonzales, C.; Schlegel, H. B. *J. Phys. Chem.* **1990**, *94*, 5523–5527.
- (27) Miertus, S.; Scrocco, E.; Tomasi, J. *Chem. Phys.* **1992**, *55*, 117–129.
- (28) Miertus, S.; Tomasi, J. *Chem. Phys.* **1982**, *65*, 239–245.
- (29) Cossi, M.; Barone, V.; Cammi, R.; Tomasi, J. *Chem. Phys. Lett.* **1996**, *255*, 327–335.
- (30) Park, H.; Zhang, K.; Ren, Y.; Nadji, S.; Sinha, N.; Taylor, J. S.; Kang, C. *Proc. Natl. Acad. Sci. U.S.A.* **2002**, *99*, 15965–15970.
- (31) Dapprich, S.; Komáromi, I.; Byun, K. S.; Morokuma, K.; Frisch, M. J. *J. Mol. Struct.: THEOCHEM* **1999**, *462*, 1–21.
- (32) Vreven, T.; Byun, K. S.; Komáromi, I.; Dapprich, S.; Montgomery, J. A., Jr.; Morokuma, K.; Frisch, M. J. *J. Chem. Theory Comput.* **2006**, *2*, 815–26.
- (33) Maseras, F.; Morokuma, K. *J. Comput. Chem.* **1995**, *16*, 1170–79.
- (34) Frisch, M. J.; Trucks, G. W.; Schlegel, H. B.; Scuseria, G. E.; Robb, M. A.; Cheeseman, J. R.; Scalmani, G.; Barone, V.; Mennucci, B.; Petersson, G. A.; Nakatsuji, H.; Caricato, M.; Li, X.; Hratchian, H. P.; Izmaylov, A. F.; Bloino, J.; Zheng, G.; Sonnenberg, J. L.; Hada, M.; Ehara, M.; Toyota, K.; Fukuda, R.; Hasegawa, J.; Ishida, M.; Nakajima, T.; Honda, Y.; Kitao, O.; Nakai, H.; Vreven, T.; Montgomery, J. A., Jr.; Peralta, J. E.; Ogliaro, F.; Bearpark, M.; Heyd, J. J.; Brothers, E.; Kudin, K. N.; Staroverov, V. N.; Kobayashi, R.; Normand, J.; Raghavachari, K.; Rendell, A.; Burant, J. C.; Iyengar, S. S.; Tomasi, J.; Cossi, M.; Rega, N.; Millam, N. J.; Klene, M.; Knox, J. E.; Cross, J. B.; Bakken, V.; Adamo, C.; Jaramillo, J.; Gomperts, R.; Stratmann, R. E.; Yazyev, O.; Austin, A. J.; Cammi, R.; Pomelli, C.; Ochterski, J. W.; Martin, R. L.; Morokuma, K.; Zakrzewski, V. G.; Voth, G. A.; Salvador, P.; Dannenberg, J. J.; Dapprich, S.; Daniels, A. D.; Farkas, Ö.; Foresman, J. B.; Ortiz, J. V.; Cioslowski, J.; Fox, D. J. *Gaussian 09, Revision B.01*; Gaussian, Inc.: Wallingford CT, 2009.
- (35) Protein Data Bank www.rcsb.org. See also ref 30.
- (36) Mashimo, S.; Kuwabara, S.; Yagihara, S.; Higasi, K. *J. Phys. Chem.* **1987**, *91*, 6337–6338.
- (37) Makov, G.; Nitzan, A. *J. Phys. Chem.* **1994**, *98*, 3459–3466. In this reference, evidence is given for assuming a value for the high-frequency dielectric constant of ~2.
- (38) Aflatoonni, K.; Gallup, G. A.; Burrow, P. D. *J. Phys. Chem. A* **1998**, *102*, 6205–6207.
- (39) We use the vertical IP to make this estimate because the photon absorption event occurs on a time scale that is short relative to motions of the OG's nuclei.
- (40) For example, our reorganization energy and $|\Delta G|$ estimates are considerably larger than those reported in Davis, W. B.; Hess, S.; Neydenova, I.; Haselsberger, R.; Ogródniczak, A.; Newton, M. D.; Michel-Beyerle, M.-E. *J. Am. Chem. Soc.* **2002**, *124*, 2422–2423. In ref 1, the authors quote a value of $\Delta G_{\text{FeT}} = -1.3$ eV. If this value were to be used in conjunction with our value for Δ of 1.4 eV, we would obtain a reorganization energy of 2.7 eV and an activation energy of $E_{\text{FeT}} = 0.18$ eV..
- (41) Middleton, C. T.; de La Harpe, K.; Su, C.; Law, Y. K.; Crespo-Hernandez, C. E.; Kohler, B. *Annu. Rev. Phys. Chem.* **2009**, *60*, 217–239.
- (42) Schwalb, N. K.; Temps, F. *J. Am. Chem. Soc.* **2007**, *129*, 9272–9273.
- (43) de La Harpe, K.; Crespo-Hernandez, C. E.; Kohler, B. *J. Am. Chem. Soc.* **2009**, *131*, 17557–17559.
- (44) Kumar, A.; Sevilla, M. D. *Chem. Rev.* **2010**, *110*, 7002–7023.
- (45) Sobolewski, A. L.; Domcke, W. *Phys. Chem. Chem. Phys.* **2004**, *6*, 2763–2771.
- (46) The rates for the A_{18} and A_{13} cases were below their detection threshold, so we report them as 0.
- (47) Takaya, T.; Su, C.; de La Harpe, K.; Crespo-Hernandez, C. E.; Kohler, B. *Proc. Natl. Acad. Sci.* **2008**, *105*, 10285–10290.
- (48) Giese, B. *Curr. Opin. Chem. Biol.* **2002**, *6*, 612–618.
- (49) Davis, D.; Vysotskiy, V. P.; Sajeev, Y.; Cederbaum, L. S. *Angew. Chem., Int. Ed.* **2011**, *50*, 4119–4122.
- (50) Durbeej, B.; Eriksson, L. A. *J. Am. Chem. Soc.* **2000**, *122*, 10126–10132.
- (51) Voityuk, A. A.; Michel-Beyerle, M. E.; Rösch, N. *J. Am. Chem. Soc.* **1996**, *118*, 9750–9758.
- (52) Aida, M.; Inoue, F.; Kaneko, M.; Dupuis, M. *J. Am. Chem. Soc.* **1997**, *119*, 12274–12279.
- (53) Borg, O. A.; Eriksson, L. A.; Durbeej, B. *J. Phys. Chem. A* **2007**, *111*, 2351–2361.